Cumhuriyet Sci. J., 46(2) (2025) 384-389
DOI: https://doi.org/10.17776/csj.1672170

Cumhuriyet Science Journal

| csj.cumhuriyet.edu.tr | Founded: 2002 ISSN: 2587-2680 e-ISSN: 2587-246X Publisher: Sivas Cumhuriyet University

# Superlattice Structure of Quantum Cascade Lasers: Structural and Morphological Effects of $AsH_3$ Flow

**Merve Nur Koçak [1, 3, a], İlkay Demir [2, 3, b, *]**

[1] *Department of Metallurgical and Materials Engineering, Sivas Cumhuriyet University, 58140 Sivas, Türkiye*
[2] *Department of Nanotechnology Engineering, Sivas Cumhuriyet University, 58140 Sivas, Türkiye*
[3] *Sivas Cumhuriyet University Nanophotonics Application and Research Center-CÜNAM, 58140 Sivas, Türkiye*
**Corresponding author*

**Research Article**

*History*
*Received: 09/04/2025*
*Accepted: 14/06/2025*



**ABSTRACT**

Quantum cascade lasers (QCLs) have been widely used in mid-infrared applications due to their high power, efficiency, and design flexibility. The InP-based quantum cascade lasers, particularly those utilizing In $In_{0.53}Ga_{0.47}As/In_{0.52}Al_{0.48}As$ superlattices, have been preferred for their lattice compatibility and well-established fabrication processes. However, the superlattice growth has required optimization, as relaxation mechanisms have affected structural quality beyond the critical thickness. In this study, InP-based quantum cascade lasers structures have been grown and characterized using Metal-Organic Vapor Phase Epitaxy (MOVPE). The impact of $AsH_3$ (arsine) flow rate on superlattice quality has been investigated by growing samples with flow rates of 47 sccm, 60 sccm, and 75 sccm. Structural analysis has been conducted using high-resolution X-ray diffraction (HRXRD), while atomic force microscopy (AFM) has been used to examine surface morphology. The results obtained revealed the critical role of superlattice growth parameters on the performance of quantum cascade laser devices and provided important findings for determining the optimal $AsH_3$ flow rate. This study contributes to the improvement of growth processes of InP-based quantum cascade laser structures, leading to improved semiconductor laser performance.

***Keywords:*** MOVPE, epitaxy, InGaAs/InAlAs superlattice, $AsH_3$ effect, QCL

[a] mervenurkocak@cumhuriyet.edu.tr https://orcid.org/0000-0002-4913-5614
[b] idemir@cumhuriyet.edu.tr https://orcid.org/0000-0002-2224-989X

## Introduction

Even though semiconductor laser technology has been around for a while, it wasn't until the introduction of Quantum Cascade Laser (QCL) technology that compact semiconductor lasers with comparatively high power density in the mid-wave infrared (MWIR), long-wave infrared (LWIR), and far-infrared (FIR) spectral regions could be developed [1-3]. In 1994, QCL was invented, and in 1997, it was first shown to function as a single mode [4, 5]. QCLs have garnered considerable interest in recent years for mid-wave infrared (MWIR) and long-wave infrared (LWIR) applications due to their wavelength tunability, compact dimensions, continuous-wave functionality at ambient temperature, elevated optical power output, and minimal cooling demands [6, 7]. QCLs are utilized in several applications including explosive detection, infrared countermeasures, food safety, greenhouse gas monitoring, breath analysis, blood urea measurement, and free-space optical communication [8-10]. Given these remarkable applications, QCLs are important both for the present and the future.

The architecture of a QCL has numerous repeated quantum wells and barriers, enabling intersubband emission. The key advantage of this feature is that the emitted radiation wavelength of QCL is not limited to the bandgap of the material. In superlattice (SL) material systems, energy levels and sub-band transitions can be controlled depending on the material composition and thickness of the layers, and thus light emission at the targeted wavelength can be achieved by adjusting only the quantum well and barrier thicknesses [3, 11]. QCLs have a relatively thick active core obtained by growing hundreds of layers on top of each other. The most important requirement is very precise control of the growth process. Small variations in both alloy ratios and the thickness of the wells and barriers can degrade laser performance. For this reason, Molecular Beam Epitaxy (MBE) and Metalorganic Vapor Phase Epitaxy (MOVPE) growth methods are commonly employed for QCL fabrication. Samples grown with MOVPE have lower background doping levels due to the use of high-purity precursors and highly controlled flows, and are preferred because they are suitable for mass production [12]. InP based QCL active cores are generally designed using InGaAs wells and InAlAs barrier layers in the literature due to their lattice compatible growth capabilities [13, 14]. Optimization of quantum wells and barriers is of great importance to provide precise control. There are many parameters affecting wells and barriers. These are growth temperature, growth pressure, growth ratio, flow rates of group V and group III gases are important parameters for QCL optimization. The conditions required for high quality growth of InGaAs and InAlAs are different from each other, making optimization of SL structured active core even more difficult [15-18]. In order to obtain these layers with desired concentrations and thicknesses, initially, single-layer growth is performed. However, since layers much thicker than SL structures are grown during single layer optimization, critical thickness is exceeded and relaxation mechanism comes into play. Therefore, optimization of devices with SL structures should be verified with SL optimizations. In this study, $AsH_3$ flow investigations were conducted on SL structures intended for use in QCL structure. SL structures were grown using MOVPE. Alloy concentration and thickness of the structure were obtained by high resolution X-ray diffraction method. Also, the change in surface morphology was investigated by atomic force microscopy.

## Materials and Methods

The samples to be examined in this paper were grown in an AIXTRON 200-4 RF/S horizontal reactor using the Metalorganic Chemical Vapor Deposition Method (MOCVD). The InGaAs/InAlAs SL structure was grown on InP substrate with (100) orientation. The SL was grown for 30 periods with the InGaAs layer of 5 nm and InAlAs layer of 5 nm in a lattice matched manner. TMIn, TMGa and TMAl metalorganic sources were used to grow the samples. A $PH_3$ hybrid source was used to prevent the P atoms escaping from the surface while heating the substrate and an $AsH_3$ hybrid source was used to grow the SL layers. During the growth of the three samples, TMIn, TMGa and TMAl flows were kept constant and the $AsH_3$ flow was varied. Table 1 shows the $AsH_3$ flows of the samples. To analyze the effect of $AsH_3$ flow on the properties of the lattice-matched SL, its structural properties were characterized using Rigaku High Resolution XRD at room temperature. The surface morphology was analyzed using Atomic Force Microscopy.

## Results and Discussion

XRD is an important method for structural characterization of SL. In semiconductor devices such as QCL, where thin and multi-repeat structures such as SL structure are used, the thickness and concentration are determined by XRD method with SL optimization. The out-of-plane θ-2θ scans obtained by HR-XRD were modeled using GlobalFit software [19] and the thicknesses of the SL layers and In concentrations were determined. Table 2 shows the results of the SL structures of Sample C, Sample N and Sample M. The As atom on the surface during growth affects the In and Ga placement. This effect is more effective in strain-balanced structures and less effective in lattice-compatible structures [20]. When the results are analyzed, no serious effect on the In concentration is observed for this reason. It is seen that sample C slightly increases the In concentration, but it is not a significant increase. Even if As did not significantly affect the In concentration in lattice-matched structures, it is thought to cause alloy disordering. Alloy disorder increases the interface roughness and decreases the device performance [21].

**Table 1.** Growth parameters of the samples

| Sample Name | $AsH_3$ Flow (sccm) |
|---|---|
| C | *47* |
| N | *60* |
| M | *75* |

**Table 2.** XRD results obtained using the GlobalFit program a) Sample C, b) Sample N and c) Sample M

**a) Sample C**

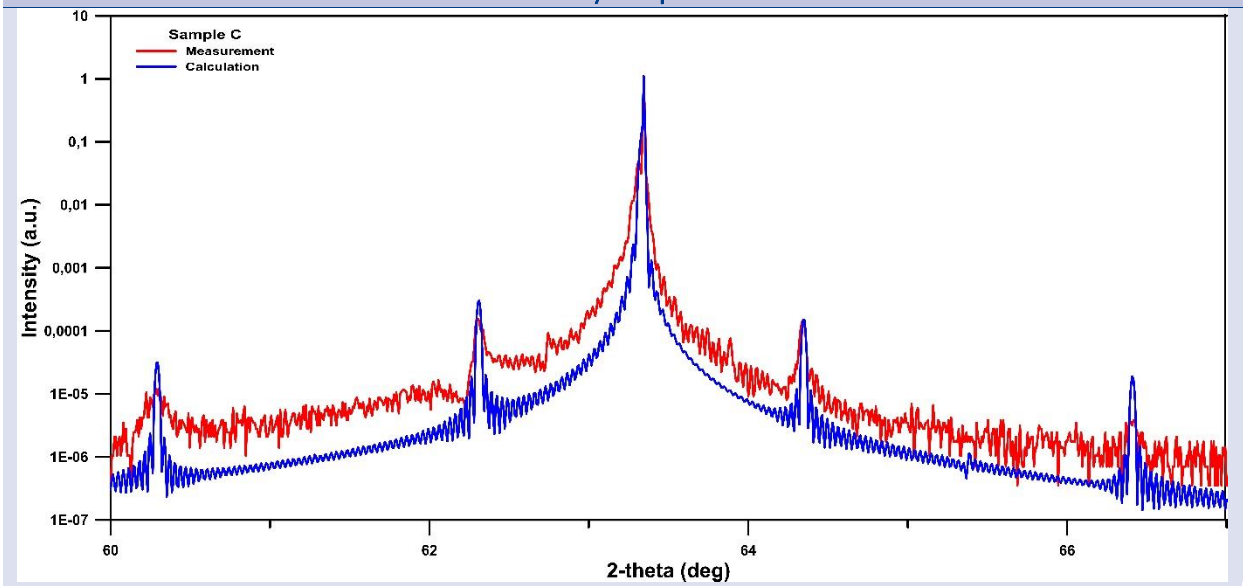


| Layer Name | In Cons. | Thickness (nm) |
|---|---|---|
| InGaAs | 0.535 | 5.11 |
| InAlAs | 0.524 | 5.05 |

**b) Sample N**

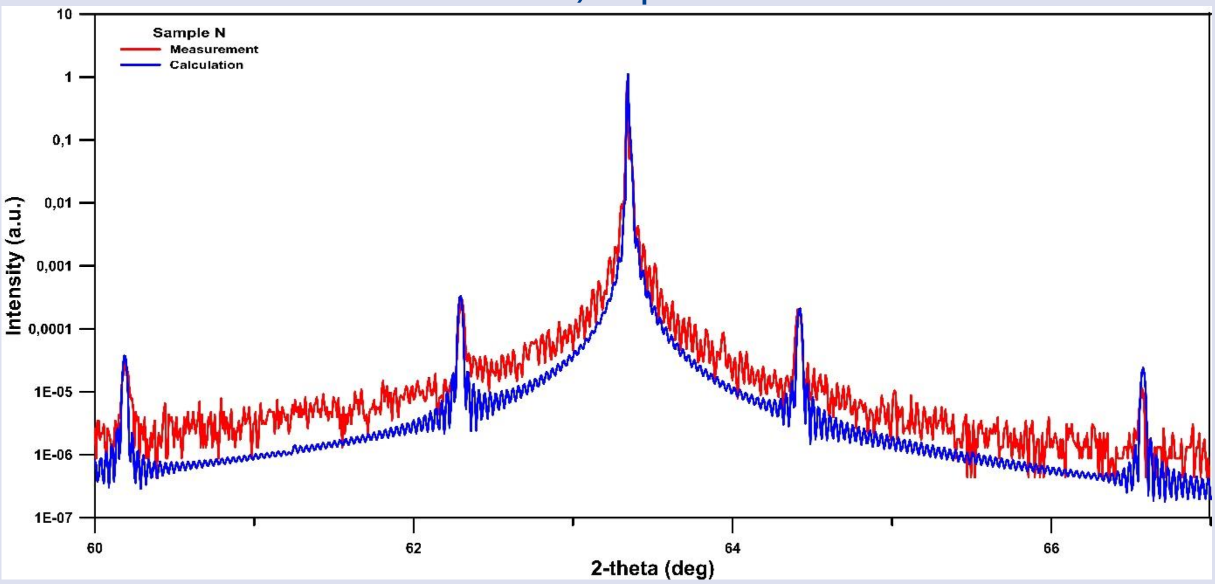


| Layer Name | In Cons. | Thickness (nm) |
|---|---|---|
| InGaAs | 0.531 | 4.87 |
| InAlAs | 0.521 | 4.88 |

**c) Sample M**

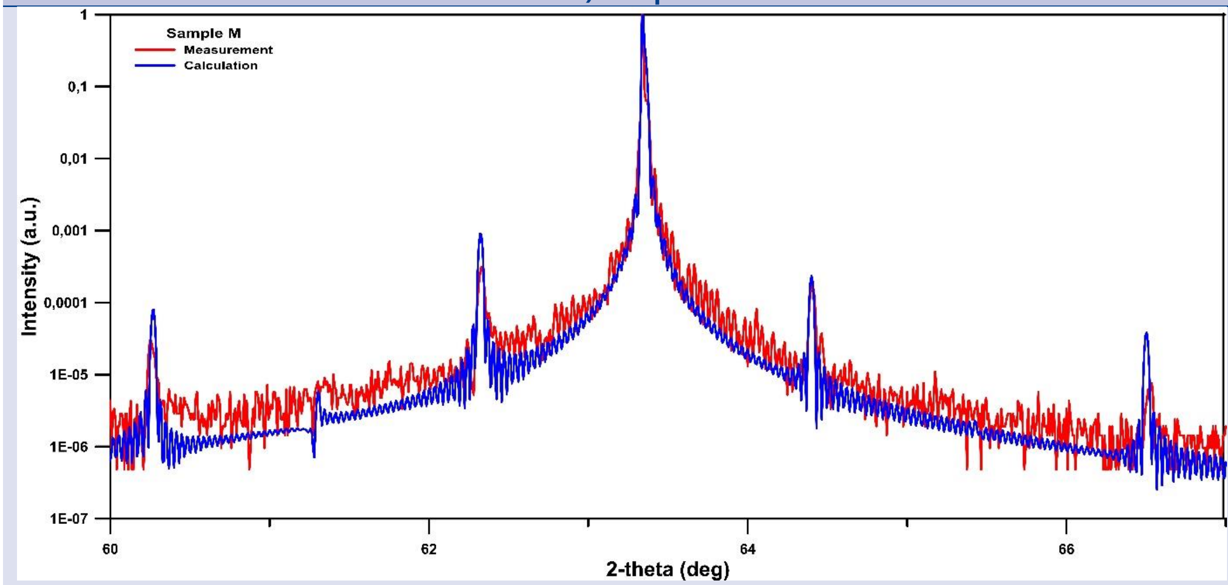


| Layer Name | In Cons. | Thickness (nm) |
|---|---|---|
| InGaAs | 0.532 | 4.9 |
| InAlAs | 0.519 | 5.08 |

In Figure 1, the XRD patterns are plotted on top of each other to facilitate comparison between the samples. When the graph is examined, slight shifts in the positions of the SL peaks are observed between the samples. As can be seen from the layer thicknesses presented in Table 2, differences in the amount of As flow affected the layer thicknesses to a certain extent. Firstly, when the -1st SL peaks marked in red are examined, slight distortions are observed in the peak shapes of Sample C and Sample M, although there is no significant difference. When the ±2nd SL peaks, marked in pink and green, were analyzed, it was found that the peaks of Sample C were significantly broadened. In addition, the 2nd SL peak of Sample M (green marking) has a lower intensity and a relatively more irregular peak shape compared to Sample N. In Sample C, the relatively low $AsH_3$ flow likely caused incomplete group-V coverage during layer transitions, promoting interface grading and compositional fluctuations. It is considered that the $AsH_3$ flow rate may have been insufficient to prevent the desorption of As atoms from the growing surface [22]. As a result, the lack of $AsH_3$ leads to a group-III-rich surface environment, which in turn deteriorates the crystal quality. These effects result in broader and asymmetric satellite peaks in

HRXRD. Conversely, in Sample M, excessive $AsH_3$ flow is thought to suppress atomic mobility, thereby limiting the formation of sharp transitions between quantum wells and barriers. This leads to weaker and irregular higher-order satellite peaks. The symmetric and well-resolved SL peaks observed in Sample N indicate sharp interfaces and a well-preserved superlattice periodicity, reflecting optimal $AsH_3$ flow conditions during growth. Based on the structural analysis, Sample N is considered to have optimal growth conditions.

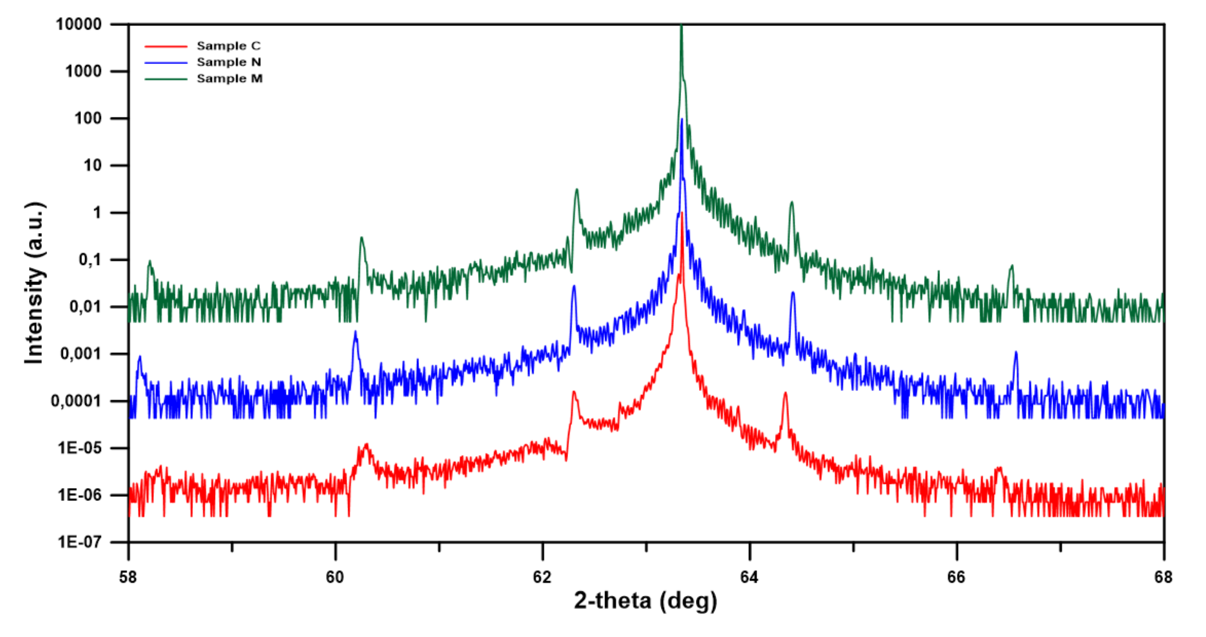


Figure 1. Comparative representation of XRD graphs of Sample C, Sample N and Sample M. The XRD data was shifted up for clarity.

Figure 2 shows the AFM images and Figure 3 shows the RMS plot obtained from these images. The AFM images show distinct linear step-flow-like structures in Sample N where optimal surface mobility is achieved. In cases where atoms are bound in the right place and have sufficient time and kinetic energy, efficient surface migration of group III atoms allows growth to occur in a step-flow mode [23]. When optimal epitaxial growth conditions are met, the step-flow mode dominates. The surface morphology of Sample C and Sample M shows a less ordered appearance. The low flow of AsH3 in Sample C caused a lack of As atoms on the surface, resulting in an inhomogeneous distribution. Unsuitable conditions lead to surface defects and problems in the proper bonding of elements to the surface [19]. As the $AsH_3$ flow increases, the movement of group III atoms on the surface decreases, reducing surface migration. Atoms that cannot move sufficiently on the surface cause disordered structures and increase the RMS. The $AsH_3$ flow should be high enough to find a place on the surface to hold In, Ga and Al atoms and low enough for group III atoms to move on the surface [21]. Sample N has both a low RMS value and a step-flow mode surface morphology.

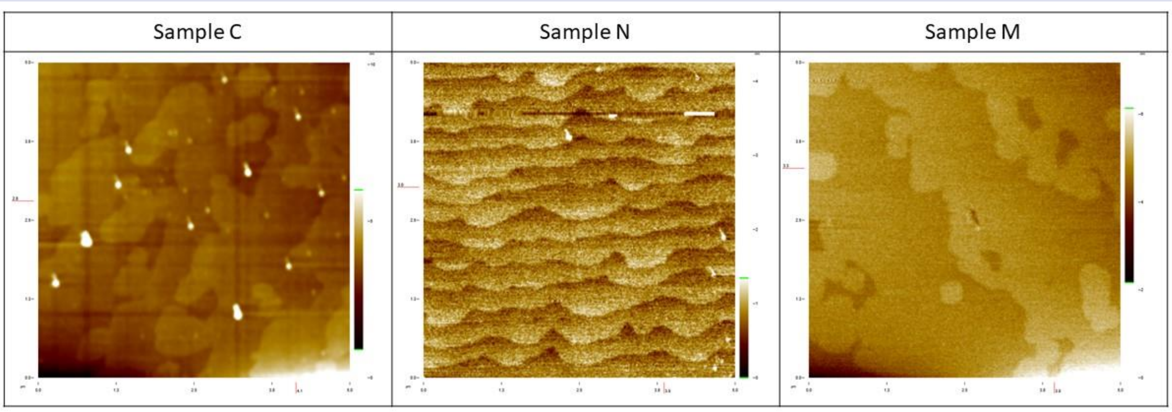


Figure 2. AFM images of samples (5um x 5um)

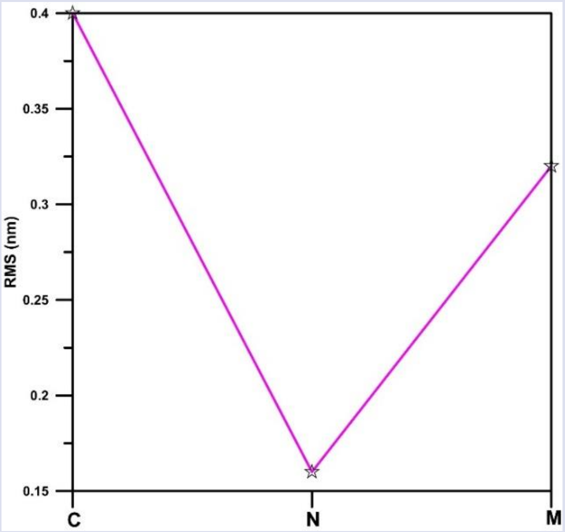

Figure 3. RMS values of the samples

## Conclusion

In this study, the effects of $AsH_3$ flow amount on the structural and surface morphology within the scope of SL optimization of QCL structures were investigated. As a result of characterization studies using HR-XRD measurements and AFM analyses, it was observed that the $AsH_3$ flow amount had a significant effect on the crystal quality and surface smoothness of SL structures.

HRXRD measurements showed that $AsH_3$ flow directly affects the SL peak shapes. In addition, AFM analysis confirmed the changes in surface morphology and showed that the step-flow growth mechanism becomes dominant under optimal $AsH_3$ flow conditions. The results show that the $AsH_3$ flow rate must be carefully controlled to achieve optimal crystal quality and surface smoothness in SL structures. In the absence of optimal growth conditions, insufficient or excessive $AsH_3$ flow rates can lead to surface and alloy disordered and consequent structural distortions that can adversely affect laser performance. In conclusion, the $AsH_3$ flow parameter plays a critical role in SL optimization in InP-based QCL growth, and determining the appropriate growth conditions is an important step in improving the performance of SL structures

## Conflicts of interest

There are no conflicts of interest in this work.

## Acknowledgement

This work is based on results obtained during the ongoing Ph.D. thesis of the first author, titled “Development of Short- and Mid-Wavelength Quantum Cascade Lasers”. Merve Nur Koçak is supported by the YÖK (Council of Higher Education) 100/2000 Ph.D. Scholarship Program and The Scientific and Technological Research Council of Turkey (TÜBİTAK) 2211/A Program. This study is supported by the Scientific Research Project Fund of Sivas Cumhuriyet University, Turkey, under Project No. MRK-2024-004, and TÜBİTAK under Project No. 22AG074.

## References


[1] Demir I., Elagoz S., Interruption time effects on InGaAs/InAlAs superlattices of quantum cascade laser structures grown by MOCVD, *Superlattices Microstruct.,* 100 (2016) 723-729.

[2] Perkitel I., Demir I., Effect of Si-doped and undoped inter-layer transition time on the strain-compensated InGaAs/InAlAs QCL active region grown with MOVPE, *J. Mol. Struct.,* 1272 (2023) 134203.

[3] Lee W.J., Sohn W.B., Shin J.C., Han I.K., Kim T.G., Kang J., Growth of InGaAs/InAlAs superlattices for strain balanced quantum cascade lasers by molecular beam epitaxy, *J. Cryst. Growth*, 614 (2023) 127233.

[4] Faist J., Capasso F., Sivco D.L., Sirtori C., Hutchinson A.L., Cho A.Y., Quantum cascade laser, *Science*, 264 (5158) (1994) 553-556.

[5] Tian W., Zhang D.L., Zheng X.T., Yang R.K., Liu Y., Lu L.D., Zhu L.Q., MBE growth and optimization of the InGaAs/InAlAs materials system for quantum cascade laser, *Front. Mater*., 9 (2022) 1050205.

[6] Wysocki G., Curl R.F., Tittel F.K., Maulini R., Bulliard J.M., Faist J., Widely tunable mode-hop free external cavity quantum cascade laser for high resolution spectroscopic applications, *Appl. Phys. B,* 81 (2005) 769-777.

[7] Yoshinaga H., Mori H., Hashimoto J.I., Tsuji Y., Murata M., Katsuyama T., Low Power Consumption (<1 W) Mid-Infrared Quantum Cascade Laser for Gas Sensing, *SEI Tech. Rev.,* 79 (2014) 112-115.

[8] Li J., Parchatka U., Fischer H., Development of field-deployable QCL sensor for simultaneous detection of ambient N2O and CO, Sens. *Actuators B Chem.,* 182 (2013) 659-667.

[9] Zhang M., Yeow J.T., Nanotechnology-Based Terahertz Biological Sensing: A review of its current state and things to come, *IEEE Nanotechnol. Mag.,* 10 (3) (2016) 30-38.

[10] Kosterev A., Wysocki G., Bakhirkin Y., So S., Lewicki R., Fraser M., Curl R.F., Mid-infrared quantum cascade lasers, *Proc. SPIE*, 10974 (2018) 59-70.

[11] Lee W.J., Seo J., Shin J.C., Han I.K., Kim T.G., Kang J., Interfacial characteristics dependence on interruption times in InGaAs/InAlAs superlattice grown by molecular beam epitaxy, *J. Alloys Compd.,* 1006 (2024) 176297.

[12] Koçak M.N., Pürlü K.M., Perkitel I., Altuntaş İ., Demir İ., In-situ and ex-situ face-to-face annealing of epitaxial AlN, *Vacuum,* 203 (2022) 111284.

[13] Bugajski M., Pierścińska D., Gutowski P., Pierściński K., Sobczak G., Janus K., Kuźmicz A., Mid-infrared quantum cascade lasers, Laser Technol, *Progress Appl. Lasers, Proc. SPIE*, 10974 (2018) 59-70.

[14] Wang C.A., Goyal A.K., Menzel S., Calawa D.R., Spencer M., Connors M.K., Capasso F., High power (>5 W) λ~9.6 µm tapered quantum cascade lasers grown by OMVPE, *J. Cryst. Growth*, 370 (2013) 212-216.

[15] Demir I., Altuntas I., Elagoz S., Arsine flow rate effect on the low growth rate epitaxial InGaAs layers, *Semiconductors*, 55 (10) (2021) 816-822.

[16] Welch D.F., Wicks G.W., Eastman L.F., Parayanthal P., Pollak F.H., Improvement of optical characteristics of Al0.48In0.52As grown by molecular beam epitaxy, *Appl. Phys. Lett.,* 46 (2) (1985) 169-171.

[17] Kurihara K., Takashima M., Sakata K., Ueda R., Takahara M., Ikeda H., Shimoyama K., Phase separation in InAlAs grown by MOVPE with a low growth temperature, *J. Cryst. Growth,* 271 (3-4) (2004) 341-347.

[18] Bass S.J., Barnett S.J., Brown G.T., Chew N.G., Cullis A.G., Pitt A.D., Skolnick M.S., Effect of growth temperature on the optical, electrical and crystallographic properties of epitaxial indium gallium arsenide grown by MOCVD in an atmospheric pressure reactor, *J. Cryst. Growth*, 79 (1-3) (1986) 378-385.

[19] Konya T., X-ray thin-film measurement techniques. X-ray reflectivity measurement, *The Rigaku Journal*, 25 (2) (2009) 1-8.

[20] Zhang S., Zhu L., Lu L., Cui J., Jia H., Du S., Li M., Effect of the V/III Ratio on the Quality of Strain-Balanced GaInAs/AlInAs Superlattices in Quantum Cascade Lasers, *Opt. Mater.,* (2025) 116882.

[21] Franckié M., Winge D.O., Wolf J., Liverini V., Dupont E., Trinité V., Wacker A., Impact of interface roughness distributions on the operation of quantum cascade lasers, *Opt*. Express, 23 (4) (2015) 5201-5212.